

# Novel synthesis of phase-pure nano-particulate anatase and rutile TiO<sub>2</sub> using TiCl<sub>4</sub> aqueous solutions

Hengbo Yin, Yuji Wada, Takayuki Kitamura, Takayuki Sumida, Yasuchika Hasegawa and Shozo Yanagida\*

Material and Life Science, Graduate School of Engineering, Osaka University, Yamada-oka, Suita, Osaka, 565-0871, Japan. E-mail: yanagida@chem.eng.osaka-u.ac.jp

Received 27th June 2001, Accepted 22nd October 2001  
First published as an Advance Article on the web 6th December 2001

Phase-pure anatase TiO<sub>2</sub> nanocrystallites ranging from 2 to 10 nm in size were synthesized directly from a TiCl<sub>4</sub> aqueous solution using citric acid as an additive. Citric acid was found to play a decisive role in stabilizing the TiCl<sub>4</sub> aqueous solution, leading to the selective formation of the anatase TiO<sub>2</sub> nanocrystallites in hydrothermal autoclaving. On the other hand, hydrothermal autoclaving of the rutile TiO<sub>2</sub> embryos prepared by room-temperature peptization of the TiCl<sub>4</sub> aqueous solution gave rod-like rutile TiO<sub>2</sub> nanocrystallites (14–17 × 22–33 nm) under neutral conditions. The presence of KCl or NaCl enhanced the crystal growth of the rutile embryos in the hydrothermal process.

## Introduction

Titania (TiO<sub>2</sub>) nanocrystallites can be used as a photocatalyst for the degradation of a variety of toxic chemicals and as a promising electrode material in dye-sensitized solar cells.<sup>1–4</sup> The crystal structure, morphology and chemical species on the surface that are derived from the starting materials play important roles in the photophysical and photochemical performances of the nanocrystallites. It is found that photoelectron transfer at the interface between TiO<sub>2</sub> nanocrystallites and substrates is strongly affected by the crystal surface and surface morphology.<sup>5,6</sup> For comparison of the characteristics of phase-pure TiO<sub>2</sub> nanocrystallites with comparable morphology, facile and novel syntheses of nano-sized anatase and rutile TiO<sub>2</sub> are worth investigation.<sup>7</sup>

Since TiCl<sub>4</sub> is commercially available and low cost, synthesis of TiO<sub>2</sub> using TiCl<sub>4</sub> is well known as exemplified by hydrothermal methods,<sup>8–10</sup> and the combustion synthesis of P-25.<sup>11</sup> As for hydrothermal synthesis using TiCl<sub>4</sub>, the experimental conditions are very harsh: there are also drawbacks, for example, high TiCl<sub>4</sub> concentration leads to the formation of hair-like and aggregated rutile TiO<sub>2</sub> while low TiCl<sub>4</sub> concentration results in the concurrent formation of anatase and rutile phase TiO<sub>2</sub>.<sup>8</sup> As reported in our preceding paper,<sup>12</sup> we elucidated that amorphous TiO<sub>2</sub> prepared by neutralization of a dilute TiCl<sub>4</sub> aqueous solution with a Na<sub>2</sub>CO<sub>3</sub> aqueous solution is a useful starting material for the selective synthesis of phase-pure anatase and rutile TiO<sub>2</sub> nanocrystallites. In addition, hydrogen fluoride and citric acid were found to play a decisive role in the hydrothermal crystal growth of amorphous TiO<sub>2</sub> to phase-pure anatase and rutile nanocrystallites, respectively.

During the investigation, we have found that citric acid suppresses the hydrolysis of TiCl<sub>4</sub> aqueous solution at room temperature, and, on the other hand, room temperature peptization of a highly concentrated TiCl<sub>4</sub> aqueous solution gives rutile nanoparticles as embryos. These findings prompted us to synthesize phase-pure anatase or rutile nanocrystallites by hydrothermal methods using TiCl<sub>4</sub> aqueous solution or rutile TiO<sub>2</sub> embryos as starting materials. We now report a novel method for the synthesis of phase-pure TiO<sub>2</sub> nanocrystallites starting from TiCl<sub>4</sub> aqueous solution.

## Experimental

### Synthesis of anatase nanocrystallites

A 50 mL portion of TiCl<sub>4</sub> aqueous solution (Ti 16.5 wt%, guaranteed reagent grade from Wako Pure Chemical Industries) was added dropwise into 250 mL of ice-water under vigorous stirring to obtain a diluted TiCl<sub>4</sub> aqueous solution (0.89 M, pH 0.23). Then 40 g of citric acid was added resulting in a clear solution which was heated in a Teflon-lined autoclave at 220 °C for 2 or 4 h. The as-prepared samples are denoted AC1 and AC2, respectively. For comparison, a sample AC3 was prepared in the absence of citric acid under the same conditions as AC1.

### Synthesis of rutile nanocrystallites

A 100 mL portion of TiCl<sub>4</sub> aqueous solution (Ti 16.5 wt%, guaranteed reagent grade from Wako) was added to 300 mL of ion-exchanged water at room temperature under vigorous stirring to obtain a diluted TiCl<sub>4</sub> aqueous solution (1.34 M, pH < 0) which was peptized at 55 °C for 6 h. The as-prepared precipitate (denoted R01) was washed with ion-exchanged water until the conductance of the filtrate was decreased to 20 mS m<sup>-1</sup>. The sample R01 was then added to ion-exchanged water, NaCl (3 M) aqueous solution, or a KCl (3 M) aqueous solution, to make a suspension of volume 200 mL, which was autoclaved at 220 °C for 8 h. The samples are denoted R02, R03 and R04, corresponding to pure water, NaCl or KCl aqueous solution as reaction media for the hydrothermal treatment of R01.

### Characterization

The crystallinities of the peptized and autoclaved samples were characterized by powder X-ray diffraction (XRD) with a Rigaku Model Dmax 2000 diffractometer using Cu-K $\alpha$  radiation ( $\lambda = 1.54056 \text{ \AA}$ ) at 50 kV and 150 mA by scanning at 2° (2 $\theta$ ) min<sup>-1</sup>. To determine the pseudo-average particle size of rutile TiO<sub>2</sub> crystallites to allow comparison of the effect of preparation conditions on the crystal growth, Scherrer's equation ( $D = K\lambda/(B\cos\theta)$ ) was applied according to XRD peak (110) broadening, where the value of  $K$  was taken as 0.9,<sup>12</sup> and  $B$  is the full width of the diffraction line at half of the

maximum intensity. The morphology and size measurements of the anatase TiO<sub>2</sub> nanocrystallites were determined by transmission electron microscopy (TEM) with a Hitachi H-800ss electron microscope at 300 kV. TEM measurements for the rutile TiO<sub>2</sub> samples were carried out with a JEM-2010 (JEOL) electron microscope at 200 kV. TEM samples were prepared by dropping a TiO<sub>2</sub> aqueous suspension onto a copper grid covered by a thin layer of carbon.

The dynamic light scattering (DLS) technique using an Otsuka electronics DLS-700 instrument was used to observe the effect of citric acid on the hydrolysis process of TiCl<sub>4</sub> at room temperature. Measured amounts of citric acid and TiCl<sub>4</sub> were added to an HCl aqueous solution of pH 0.23 to prepare a TiCl<sub>4</sub> (1 mM) or a TiCl<sub>4</sub> (1 mM)–citric acid (1 mM) aqueous solution for DLS measurement. The acidity (pH 0.23) of the solutions for DLS measurements was the same as that of the starting TiCl<sub>4</sub> and citric acid solution for the preparation of the samples AC1 and AC2 so as to validate comparisons. The prepared TiCl<sub>4</sub> (1 mM) or TiCl<sub>4</sub> (1 mM)–citric acid (1 mM) solutions were measured by the DLS technique after allowing the solutions to stand at room temperature for 2 h. The resolution of the DLS apparatus is 2 nm.

<sup>13</sup>C NMR analysis was performed on a 270 MHz JEOL EX-270 spectrometer at a frequency of 270 MHz to confirm interactions between citric acid (150 mM) and Ti<sup>4+</sup> (150 mM) under acidic conditions (DCI + D<sub>2</sub>O, pH 0.23). <sup>13</sup>C NMR chemical shifts were referenced using chloroform as an external standard.

## Results and discussion

### Citric acid-promoted synthesis of anatase TiO<sub>2</sub> nanocrystallites

When citric acid was added into a TiCl<sub>4</sub> (0.89 M, pH 0.23) aqueous solution, phase-pure anatase TiO<sub>2</sub> nanocrystallites were obtained after autoclaving at 220 °C for 2 or 4 h (Fig. 1, AC1 and AC2). The broadening of the XRD patterns of the anatase phase was decreased with increased autoclaving time (AC1 and AC2), suggesting that the degree of crystallization of anatase TiO<sub>2</sub> increases with the autoclaving time.

The TEM images show that the nanocrystallites of the samples AC1 and AC2 are nano-particulate (Fig. 2). The size distributions from the TEM images and the average particle sizes calculated by a weighted-averages method were 2–6, 4,

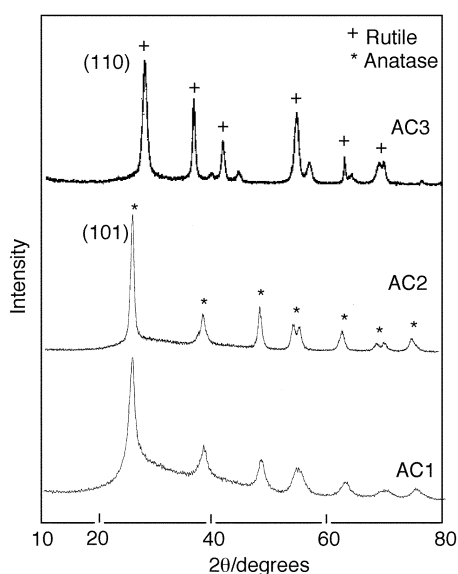
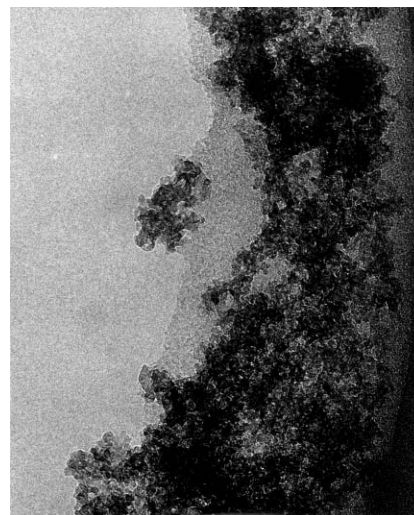
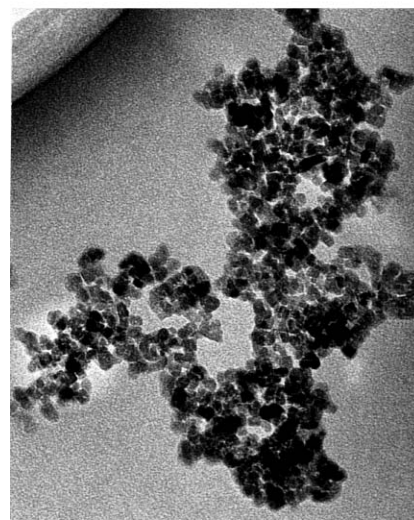


**Fig. 1** XRD patterns of the TiO<sub>2</sub> samples after autoclaving TiCl<sub>4</sub> (0.89 M, pH 0.23) aqueous solution at 220 °C for 2 (AC1, AC3) and 4 h (AC2). Citric acid was used as an additive for the preparation of samples AC1 and AC2.



AC1 20 nm



AC2 20 nm

**Fig. 2** TEM images of the anatase TiO<sub>2</sub> samples AC1 and AC2.

and 3–10, 6 nm for samples AC1 and AC2, respectively (Figs. 2 and 3). The as-prepared anatase nanoparticle size distributions were very narrow and the average particle sizes were very small when compared to anatase TiO<sub>2</sub> nanocrystallites prepared using amorphous TiO<sub>2</sub> as a starting material and HF/HCl as acid catalysts as reported in our preceding paper.<sup>12</sup>

In the absence of citric acid, rutile TiO<sub>2</sub> was exclusively formed (Fig. 1, AC3). The TEM image of the sample AC3 shows that the primary hair-like rutile TiO<sub>2</sub> nanocrystallites were found to agglomerate, giving ball-like aggregates with a size of several hundred nanometers in diameter (Fig. 4).

### Hydrothermal synthesis of rutile TiO<sub>2</sub> nanocrystallites

Fig. 5 shows the XRD patterns of samples R01–R04. The hydrolysis of a TiCl<sub>4</sub> (1.34 M, pH < 0) aqueous solution at 55 °C for 6 h gave phase-pure rutile TiO<sub>2</sub> (R01) with an average particle size of 4.3 nm (determined by XRD (110 reflection)). The TEM image of sample R01 (Fig. 6) shows that the rutile TiO<sub>2</sub> is composed of rod-like secondary particles consisting of about 5 nm granular primary nanocrystallites. The rutile embryos (R01) was washed well and autoclaved in ion-exchanged water at 220 °C for 8 h. The resulting TiO<sub>2</sub> nanocrystallites (R02) were found to grow to an average size of 13.1 nm (determined by XRD (110 reflection)) with the crystal structure unchanged *i.e.* pure rutile. The TEM image of sample R02 (Fig. 6) shows that the crystallites are composed of

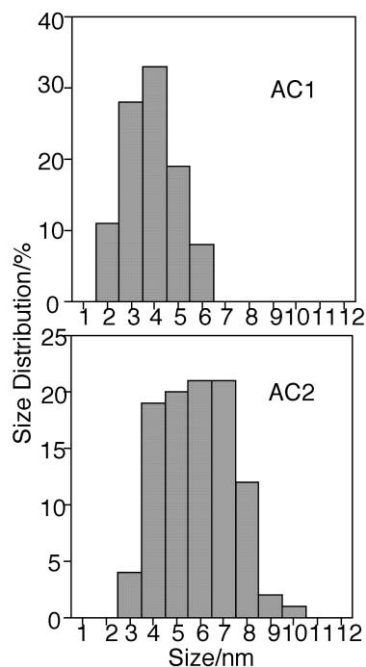


**Fig. 3** Nanocrystal size distributions of the anatase TiO<sub>2</sub> samples AC1 and AC2.

well-isolated granular and rod-like nanoparticles. The particle size distribution of the sample R02 was 6–25 × 7–52 nm, and the average particle size was 14 × 22 nm (Fig. 7).

When 3 M NaCl or KCl aqueous solution were used as the reaction medium instead of ion-exchanged water in the autoclaving at 220 °C for 8 h, the resulting TiO<sub>2</sub> nanoparticles, R03 and R04, showed a pure rutile phase with a large particle size. The pseudo-average crystalline sizes (110) calculated by Sherrer's equation were 14.5 and 15 nm for samples R03 and R04, respectively. TEM images of the samples R03 and R04 show well-isolated rod-like shapes (Fig. 6). The size distributions were in the ranges 9–32 × 16–64 and 12–36 × 16–74 nm in width and length (TEM), respectively (Fig. 7). The average particle sizes were 16 × 32 and 17 × 33 nm, respectively. The KCl system showed a tendency to give a narrower size



**Fig. 4** TEM image of the sample AC3.

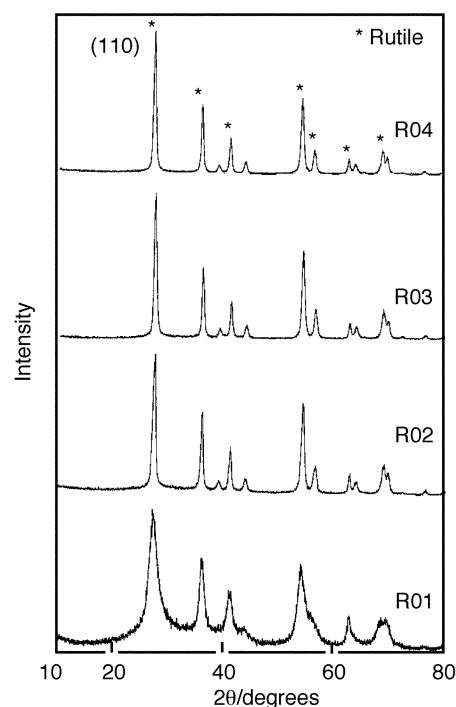


**Fig. 5** XRD patterns of rutile TiO<sub>2</sub> samples R01–R04. Sample R02 was prepared only with ion-exchanged water as reaction medium while samples R03 and R04 were treated with NaCl and KCl aqueous solutions, respectively, during hydrothermal processing of the rutile embryos.

distribution for both width and length than the NaCl system (Fig. 7).

#### Specific interaction between citric acid and Ti<sup>4+</sup>

Barboux-Doeuff and Sanchez<sup>13</sup> reported that acetate can substitute for OBU<sup>n</sup> coordinated to titanium in Ti(OBU<sup>n</sup>)<sub>4</sub> to form Ti(OBU<sup>n</sup>)<sub>3</sub>(OAc), stabilizing the sol and gel formed by hydrolysis. We proposed in our preceding paper that the chelation of citric acid to the surface of amorphous TiO<sub>2</sub> influences crystal growth to rutile TiO<sub>2</sub>.<sup>12</sup> In contrast, the present finding implies that citric acid should have ability to chelate or to coordinate to Ti<sup>4+</sup> in TiCl<sub>4</sub> aqueous solution, affecting the nucleation processes of TiO<sub>2</sub> to form anatase nanocrystallites.

As shown in the DLS measurement (Fig. 8), in the absence of citric acid, TiCl<sub>4</sub> in aqueous solution was quickly hydrolyzed to form small particles with size distribution mainly ranging from 38 to 66 nm. In the presence of citric acid, no particle formation could be detected. This fact suggested that citric acid interacts with TiCl<sub>4</sub> to prevent the rapid hydrolysis of TiCl<sub>4</sub>.

Fig. 9 shows the <sup>13</sup>C NMR spectra of a pure citric acid (150 mM) solution and a mixed solution of citric acid (150 mM) and TiCl<sub>4</sub> (150 mM). The acidity of the both solutions for the <sup>13</sup>C NMR analysis was the same as that of the reaction solution for synthesis of the samples AC1 and AC2. The four resonance signals at 43.18, 73.23, 173.23 and 176.55 ppm for the citric acid solution in the presence of TiCl<sub>4</sub> at pH 0.23 were assigned to methylene carbon (CH<sub>2</sub>), alcoholic carbon (COH), the carbons in the two terminal carboxylic acid groups (t-COOH), and a carbon in the middle carboxylic acid group (m-COOH), respectively, as reported by Tsay and Fang.<sup>14</sup> When compared to the resonance signals at 43.26, 73.23, 173.28, and 176.57 ppm (Fig. 9(b)) observed in the absence of TiCl<sub>4</sub> at a pH of 0.23, very slight upfield shifts of the carbons of CH<sub>2</sub>, t-COOH and m-COOH are evident.

Very recently, a titanium peroxo complex with citric acid with a high stability towards hydrolysis was isolated in the solid

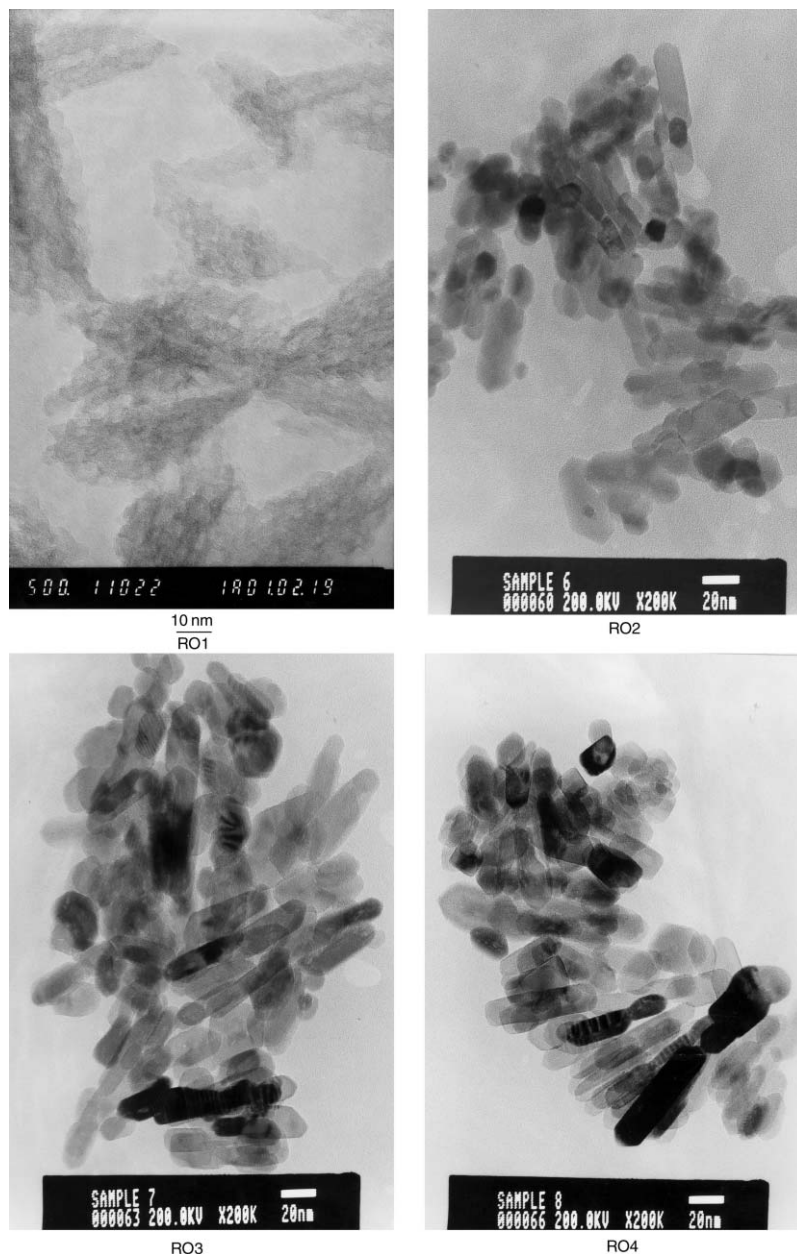


Fig. 6 TEM images of rutile  $\text{TiO}_2$  samples R01–R04.

form and the crystal structure indicated a tight coordination of titanium with t-COOH and OH.<sup>15</sup> Although no change in the signal of the carbon of COH was observed in the presence of  $\text{TiCl}_4$ , the observed upfield shifts for the  $\text{CH}_2$  and t-COOH are in agreement to some extent with the ammonium citratoperoxotitanate structure. These facts support that the t-COOH and/or m-COOH group interact with  $\text{TiCl}_4$  (or a partially hydrolyzed species), suppressing the hydrolysis of  $\text{TiCl}_4$  to  $\text{TiO}_2$  aggregates under room temperature conditions.

#### Process of anatase crystallization

Anatase and rutile  $\text{TiO}_2$  are constructed by linking  $\text{TiO}_6$  octahedra in different bonding modes.<sup>8,16,17</sup> Anatase  $\text{TiO}_2$  is built by face-sharing linking of  $\text{TiO}_6$  octahedra.<sup>16</sup> As for rutile, the sharing of two edges of each  $\text{TiO}_6$  octahedron along the *c* axis leads to chains and corner-shared bonding among chains leads to a three-dimensional crystal framework. Cheng *et al.*<sup>8</sup> explained the crystallization of anatase and rutile  $\text{TiO}_2$  by hydrolysis of a  $\text{TiCl}_4$  aqueous solution using ligand field theory. They suggested that the crystallization of anatase and rutile  $\text{TiO}_2$  should be *via* dehydration reactions between partially

hydrolyzed  $(\text{Ti}(\text{OH})_n\text{Cl}_m)^{2-}$  complexes, where  $n + m = 6$ . The coordination abilities of several ligands has been summarized below by Constable,<sup>18</sup> in the order of progressively larger crystal field splittings:  $\text{Cl}^- < \text{OH}^- < \text{C}_2\text{O}_4^{2-} < \text{H}_2\text{O}$ . The oxalate anion ligand is a stronger field ligand when compared to  $\text{Cl}^-$  and  $\text{OH}^-$  ligands while the coordination property of citrate anion should be similar to that of oxalate anion. When the effect of citric acid on the formation of anatase rather than rutile is considered, one can suppose that citrate anions substitute for the  $\text{Cl}^-$  anions in the hydrolysis process to form  $(\text{Ti}(\text{OH})_x(\text{citrate})_y\text{Cl}_z)^{n-}$  complexes, where  $4 \leq x + y + z \leq 6$ ,  $0 \leq n \leq 2$ , and related species with a higher stability than the  $(\text{Ti}(\text{OH})_n\text{Cl}_m)^{2-}$  complexes. The  $(\text{Ti}(\text{OH})_x(\text{citrate})_y\text{Cl}_z)^{n-}$  complexes and related species should be favorably polycondensed to form anatase  $\text{TiO}_2$  embryos through face-sharing linking in the highly concentrated HCl medium. The detailed effect of citrate in the citrate complexes on the nucleation process of anatase  $\text{TiO}_2$  should be worth future investigation.

The formation of small-sized anatase nanocrystallites as embryos should be due to the inhibition of the crystal growth by the coordination of the citrate anions. The narrow size distribution of the anatase nanocrystallites implied that the

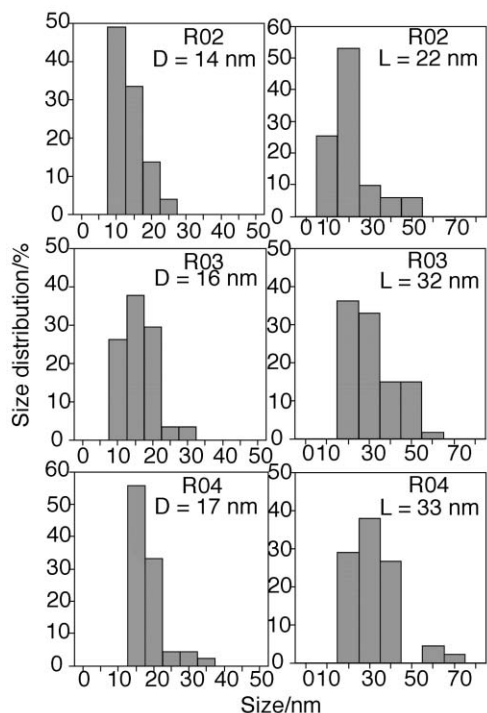


**Fig. 7** Nanocrystal size distributions of rutile TiO<sub>2</sub> samples R02–R04; *D* = nanocrystal width, *L* = nanocrystal length.

nucleation process should be finished at the early stage of the hydrothermal processing at high temperature (220 °C). Furthermore, the HCl present in the starting material TiCl<sub>4</sub> aqueous solution should catalyze not only the nucleation of anatase TiO<sub>2</sub> but also the crystal growth *via* condensation of the (Ti(OH)<sub>*x*</sub>(citrate)<sub>*y*</sub>Cl<sub>2</sub>)<sup>*n*–</sup> and related species.

### Mechanism of rutile crystallization

The hydrolysis of TiCl<sub>4</sub> will only occur to a small extent at low temperature, and a smaller number of OH ligands in the hydrolyzed (Ti(OH)<sub>*n*</sub>Cl<sub>*m*</sub>)<sup>2–</sup> complexes should decrease the rates of the nucleation and crystal growth *via* dehydration between (Ti(OH)<sub>*n*</sub>Cl<sub>*m*</sub>)<sup>2–</sup> species, leading to small-sized rutile embryos (sample R01). Autoclaving the small rutile embryos at high temperature in neutral water favors the formation of nano-particulate rutile nanocrystallites (sample R02) *via* coalescence of the small neighboring rutile embryos when compared to direct hydrothermal treatment of TiCl<sub>4</sub> aqueous solution at a high reaction temperature (sample AC3). Cheng *et al.*<sup>8</sup> also reported that the hairy rutile TiO<sub>2</sub> nanocrystallites

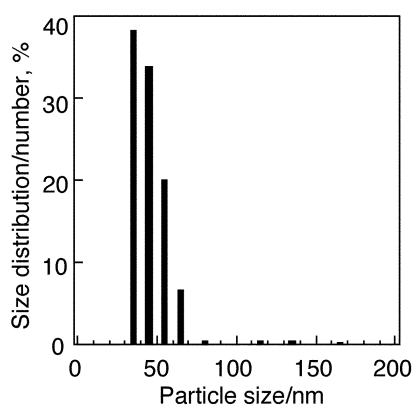


**Fig. 8** DLS spectra of a TiCl<sub>4</sub> (1 mM) aqueous solution of pH 0.23. The TiCl<sub>4</sub> aqueous solution was allowed to stand for 2 h before the DLS measurement.

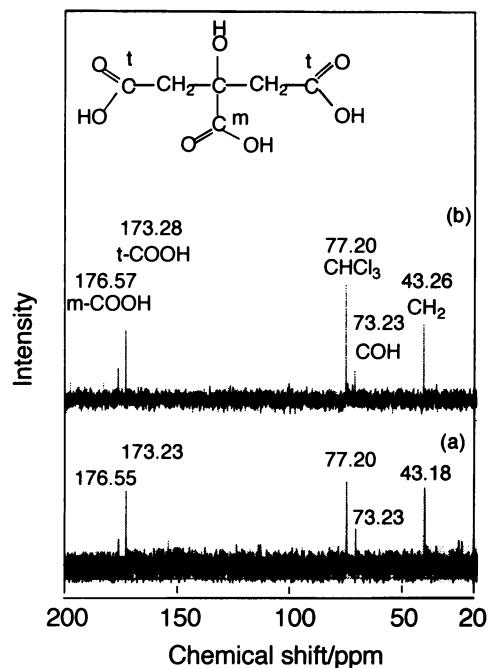


**Fig. 9** <sup>13</sup>C NMR spectra of (a) a citric acid (150 mM)–TiCl<sub>4</sub> (150 mM) solution of pH 0.23 and (b) a pure citric acid (150 mM) solution of pH 0.23; CHCl<sub>3</sub> was used as the external standard.

agglomerated to form broom-like secondary particles when TiCl<sub>4</sub> (1.4 M) was directly hydrolyzed at 220 °C for 2 h. The acidity of the reaction medium should be a critical factor to the particle agglomeration during hydrolysis of acidic TiCl<sub>4</sub> aqueous solutions. As reported by Bahnemann *et al.*,<sup>19</sup> the surface properties of TiO<sub>2</sub> could be changed by protonation as follows: TiO<sub>2</sub> + *n*H<sup>+</sup> = TiO<sub>2</sub>H<sub>*n*</sub><sup>*n*+</sup>, at pH < 3.5. The agglomeration of rutile TiO<sub>2</sub> under highly acidic conditions could be attributed to hydrogen bonding among the protonated rutile nanocrystallites. In a neutral reaction medium, however, the coordinated water molecules should suppress the agglomeration among the freshly formed rutile nanocrystallites, so leading to particulate crystal growth.

The presence of NaCl or KCl enhanced the crystal growth during the autoclaving when compared to the pure water reaction system. Yanagisawa and Ovenstone<sup>16</sup> soaked amorphous TiO<sub>2</sub> in NaCl, KCl, K<sub>2</sub>SO<sub>4</sub>, Na<sub>2</sub>SO<sub>4</sub> and NaF aqueous solutions for one week and dried the TiO<sub>2</sub> at 120 °C for 90 min. Only chloride salts were reported to enhance the crystallization of the anatase phase. They suggested that the salt effect on the crystallization should be due to the different adsorption abilities of the salt anions at the titania surface. Hence, we speculate that Cl<sup>–</sup> can coordinate to the existing rutile embryos, which should be beneficial to the coalescence among the rutile embryos. The salt-enhanced crystal growth may also be rationalized in terms of a salting-out effect. The salting-out effect should promote the surface diffusion between the coalesced small rutile embryos to form large and phase-pure nanocrystallites.

### Conclusions

Citric acid stabilizes TiCl<sub>4</sub> aqueous solution through coordination to partially hydrolyzed titanium anionic complexes, promoting the nucleation for anatase phase formation during the hydrothermal autoclaving of TiCl<sub>4</sub> aqueous solution. The coordination of citrate to the crystal surfaces may also contribute to the formation of nano-particulate anatase TiO<sub>2</sub> with smaller size and narrower size distribution. In addition, HCl present in the hydrothermal process catalyzed the fast nucleation of the anatase TiO<sub>2</sub> rather than the crystal growth,

contributing to the formation of anatase nanocrystallites with a narrower size distribution and a smaller particle size than in the previous method.<sup>12</sup>

Nano-particulate rutile TiO<sub>2</sub> nanocrystallites with rod-like shapes were prepared by hydrothermal treatment at high temperature of the rutile embryos prepared by hydrolysis of TiCl<sub>4</sub> aqueous solution at low temperature. Water as a neutral reaction medium was beneficial to the formation of the well-particulate rutile nanocrystallites. The presence of NaCl and KCl in the hydrothermal processing of rutile embryos enhanced the crystal growth *via* coalescence of the embryos.

## References

- 1 M. A. Fox and M. T. Dulay, *Chem. Rev.*, 1993, **93**, 341.
- 2 C. Kormann, D. W. Bahnemann and M. R. Hoffmann, *J. Phys. Chem.*, 1988, **92**, 5196.
- 3 D. D. Beck and R. W. Siegel, *J. Mater. Res.*, 1992, **7**, 2840.
- 4 K. Kalyanasundaram and M. Grätzel, *Coord. Chem. Rev.*, 1998, **77**, 347.
- 5 Z. Zhang, C. C. Wang, R. Zakaria and J. Y. Ying, *J. Phys. Chem. B*, 1998, **102**, 10871.
- 6 H. Zhang, R. L. Penn, R. J. Hamers and J. F. Banfield, *J. Phys. Chem. B*, 1999, **103**, 4656.
- 7 S. Kambe, K. Murakoshi, T. Kitamura, Y. Wada, S. Yanagida, H. Kominami and Y. Kera, *Sol. Energy Mater. Sol. Cells*, 2000, **61**, 427.
- 8 H. Cheng, J. Ma, Z. Zhao and L. Qi, *Chem. Mater.*, 1995, **7**, 663.
- 9 J. Moser and M. Grätzel, *J. Am. Chem. Soc.*, 1983, **105**, 6547.
- 10 M. Anpo, T. Shima, S. Kodama and Y. Kubokawa, *J. Phys. Chem.*, 1987, **91**, 4305.
- 11 S. T. Aruna and K. C. Patil, *J. Mater. Synth. Process.*, 1996, **4**, 175.
- 12 H. Yin, Y. Wada, T. Kitamura, S. Kambe, S. Murasawa, H. Mori, T. Sakata and S. Yanagida, *J. Mater. Chem.*, 2001, **11**, 1694.
- 13 S. Barboux-Doeuff and C. Sanchez, *Mater. Res. Bull.*, 1994, **29**, 1.
- 14 J. D. Tsay and T. T. Fang, *J. Am. Ceram. Soc.*, 1999, **82**, 1409.
- 15 M. Kakihana, M. Tada, M. Shiro, V. Petrykin, M. Osada and Y. Nakamura, *Inorg. Chem.*, 2001, **40**, 891.
- 16 K. Yanagisawa and J. Ovenstone, *J. Phys. Chem. B*, 1999, **103**, 7781.
- 17 M. Kiyono, *Titanium Oxides: Properties and Application*, Gihodo Press, Tokyo, 1st edn., 1991, pp. 47–49.
- 18 E. C. Constable, *Metals and Ligand Reactivity: An Introduction to the Organic Chemistry of Metal Complexes*, VCH Publishers, New York, 1996, p. 7.
- 19 D. Bahnemann, A. Henglein and L. Spanhel, *Faraday Discuss. Soc.*, 1984, **78**, 151.